JOURNAL OF GUIDANCE, CONTROL, AND DYNAMICS
Vol. 16, No. 3, May-June 1993

Robustness Evaluation of a Flexible Aircraft Control System

Mark R. Anderson*
Virginia Polytechnic Institute and State University, Blacksburg, Virginia 24061

The structured singular value analysis technique is used to generate stability and performance robustness guidelines for multivariable, flexible aircraft flight control systems. A stability augmentation and structural mode control system, designed using the same classical technique as on the original production aircraft, is evaluated to produce the new guidelines. Stability margins are computed for simultaneous gain and phase uncertainty in each of the control system feedback loops. Performance weighting filters are chosen specifically from military flying qualities specifications. The results of this research define exactly how robust a control system of this type should be, such that any performance improvements achieved using more advanced design techniques can be compared directly.

I. Introduction

RECENT advances in the development of robustness "measures," primarily from singular value and structured singular value analysis techniques, allow the controls engineer to quantify the robustness of a feedback control system. In fact, many loop-shaping control system design techniques are being considered that directly shape or minimize some measure of robustness; examples include LQG/LTR, H^2/H^∞, and μ synthesis. Unfortunately, research involved with determining exactly how robust a control system should be has not kept pace with research regarding control design techniques that claim to yield maximum performance. As a consequence, an often heard complaint about multivariable control systems is that they are overdesigned. In other words, simplicity of the control system has been sacrificed in an attempt to maximize performance far beyond the level that is actually required.

Ongoing research is beginning to reveal evaluation guidelines with regard to stability robustness. Specifications for single-loop stability margins are listed in the current military flight control system specification.[1] References 2 and 3 represent some of the few published results about computation of multiloop stability margins for production flight control systems. Other results in this area will no doubt be published in the near future as software for computation of stability robustness measures becomes more readily available.

Although nominal flight control system performance is generally specified by the military flying qualities standard,[4] performance robustness guidelines have no similar formal standard. Most existing performance robustness requirements are generalized requirements such as the often mentioned rule of thumb: "high gains at low frequency and low gains at high frequency." There are relatively few, if any, performance robustness guidelines with direct ties to flying qualities specifications.

The objective of this paper is to develop evaluation guidelines for robust stability and performance of a large, flexible aircraft. The most direct method of developing the guidelines is to study an existing, successful flight control system to determine exactly how robust it is. A multivariable flight control system for an existing aircraft is used to develop the guidelines. The aircraft model chosen for analysis is the B-1 bomber. The control system under study was designed using the same (over 20-yr old) design technique as used for the actual aircraft. Once the guidelines have been established, the performance of new and different designs can be compared directly using the analysis results.

The evaluation is carried out using the relatively new structured singular value analysis technique, with weighting filters chosen specifically to reflect design characteristics of flight control systems. The structured singular value analysis technique is quickly becoming the accepted method for measuring control system robustness. A general statement of the structured singular value analysis technique can be found in Ref. 5, and computational algorithms and examples can be found in Ref. 6. An additional attraction of using the structured singular value analysis technique is that the weighting filters developed for the analysis can also be used directly in many control system synthesis approaches such as H^∞ and μ synthesis.

II. Study Vehicle and Control System

The longitudinal-axis linear model of the B-1 aircraft, including 1 rigid-body mode and 10 elastic modes, is included in Ref. 7 and will be used for this analysis. For simplicity, only the rigid-body mode (short period) and the first two fuselage bending modes (19.5 and 39.7 rad/s) of the original model were retained. Both the elevator and forward control vane are used for control. First-order actuators are assumed, with a time constant of 1/10 s for the elevator and 1/50 s for the control vane. The flight condition is a low-level, high-speed run with altitude of 25 ft and Mach = 0.85.

The B-1 aircraft model used for this analysis can be expressed in a linear, state-space form:

$$\frac{\mathrm{d}x}{\mathrm{d}t} = Ax + Bu$$

$$y = Cx + Du$$

The model state vector is defined as x = [elevator position (rad), control vane position (rad), angle of attack (rad), pitch rate (rad/s), first bending mode (in.), second bending mode (in.), first bending mode rate (in./s), and second bending mode rate (in./s)]. The model input vector is u = [elevator command (rad), vane command (rad), and plunge gust (ft/s)]. The model output vector is y = [pitch rate c.g. (rad/s), pitch acceleration c.g. (rad/s^2), normal acceleration c.g. (g), and normal acceleration pilot (g)]. The numerical values of the linear model matrices A, B, C, and D are listed in Table 1.

A stability augmentation and structural mode control system was designed for the subject aircraft using the identical location of accelerometer and force (ILAF) concept. The ILAF design concept was developed by North American Rockwell and was successfully implemented on both the B-1 and

Presented as Paper 90-3445 at the AIAA Guidance, Navigation, and Control Conference, Portland, OR, Aug. 20-22, 1990; received Feb. 10, 1992; revision received Aug. 31, 1992; accepted for publication Sept. 4, 1992.

*Assistant Professor, Department of Aerospace and Ocean Engineering. Member AIAA.

Table 1 B-1 aircraft linear model

$A =$								
	−10.0	0	0	0	0	0	0	0
	0	−50.0	0	0	0	0	0	0
	−0.2529	−0.0035	−0.9850	0.9539	−0.0128	0.0049	−0.0001	−0.0005
	−15.7550	0.2905	−9.9701	−1.8641	−0.4931	0.4754	−0.0149	−0.0015
	0	0	0	0	0	0	1.0	0
	0	0	0	0	0	0	0	1.0
	−2971.7	−57.0	−194.1	−173.4	−380.6	37.2	−4.6	1.9
	313.9	−31.0	−1470.4	−89.7	−9.7	−1578.9	−0.4	−4.9
$B =$								
	10.0	0	0	—	—	—	—	—
	0	50.0	0	—	—	—	—	—
	0	0	−0.0010	—	—	—	—	—
	0	0	−0.0106	—	—	—	—	—
	0	0	0	—	—	—	—	—
	0	0	0	—	—	—	—	—
	0	0	−0.2061	—	—	—	—	—
	0	0	−1.5609	—	—	—	—	—
$C =$								
	0	0	0	1.0	0	0	0.0047	0.0057
	−27.9860	−0.1558	−19.2971	−3.1952	−2.3450	−8.3805	−0.0388	−0.0209
	8.4571	−0.1110	20.2640	0.6177	−1.0197	−3.3898	−0.0119	−0.0018
	−1.1958	2.7961	16.1391	−0.7979	6.2202	22.1817	0.0396	0.0134
$D =$								
	0	0	0	—	—	—	—	—
	0	0	−0.0205	—	—	—	—	—
	0	0	0.0215	—	—	—	—	—
	0	0	0.0171	—	—	—	—	—

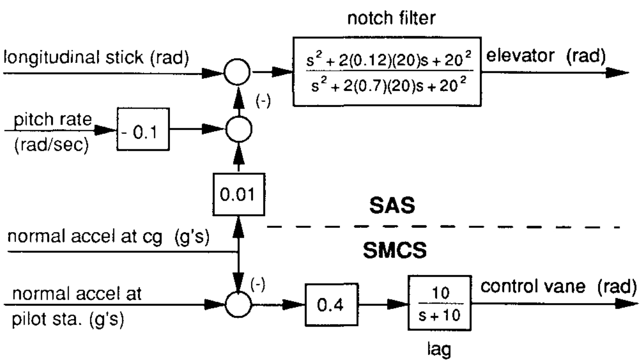

Fig. 1 SAS and SMCS for the B-1 aircraft.

XB-70 aircraft.[8] The ILAF flight control system is shown in Fig. 1. The control system consists of two parts: the stability augmentation system (SAS) and the structural mode control system (SMCS). The SAS was designed by blending a pitch rate gyro signal and the vertical acceleration signal, both from the vehicle center of mass, and feeding the resulting signal to the elevator. A notch filter is included in the SAS to reduce the effect of the first bending mode on the pilot commanded response.

The SMCS is used to reduce vibration at the cockpit of the aircraft due to turbulence and is pilot selectable. The ILAF design concept involves subtracting a vertical acceleration signal taken near the vehicle center of mass from a vertical acceleration signal taken near the cockpit. The blended signal is then fed through a lag filter, which represents a high-frequency approximation of an integrator. The blended acceleration signal is approximately integrated to a velocity signal that is fed to the control vane. This configuration sets up a root locus wherein zeros are placed at lower natural frequencies than the structural mode poles and the rigid-body mode remains relatively unaffected. Figure 2 depicts the root locus of the SMCS with the SAS elevator feedback loop already closed. The root locus in Fig. 2 represents the possible root locations due to variations in the SMCS feedback gain that acts on the blended, approximately integrated, acceleration signal and is fed back to the structural mode control vane. The root locus demonstrates that the ILAF concept will improve the damping of both the first and second bending modes, with a slight reduction in the short-period mode damping provided by the SAS loop closure. The SMCS feedback gain was chosen to increase the first bending mode damping ratio from the open-loop value of 0.13 to a closed-loop value of 0.23, whereas the second bending mode damping ratio was increased from 0.06 to 0.08. With both the SAS and SMCS loops closed, the short-period mode damping ratio was increased from an open-loop value of 0.39 to a closed-loop value of 0.54.

It is important to recognize that the ILAF concept does not yield "tight," high bandwidth feedback loops and usually results in very low feedback gains. Since the open-loop aircraft dynamics are stable and inherently provide at least acceptable flying qualities, the purpose of the SAS/SMCS is to tune the aircraft dynamics to improve the aircraft flying qualities to a satisfactory level. As noted previously, the B-1 pilot is able to turn the SMCS on and off from the cockpit. The root locus in Fig. 2 clearly shows that the SMCS gain can be set to zero without leading to instability. In addition, the root locus also shows that the SMCS gain can be increased to (positive) infinity without causing an instability. The SAS serves only to increase the short-period damping from an open-loop value of 0.39 to a value of 0.60 (with SAS loop closed and SMCS loop open). Consequently, it should come as no surprise that the SAS/SMCS has very large stability margins, a fact that will be confirmed in Sec. V of this paper.

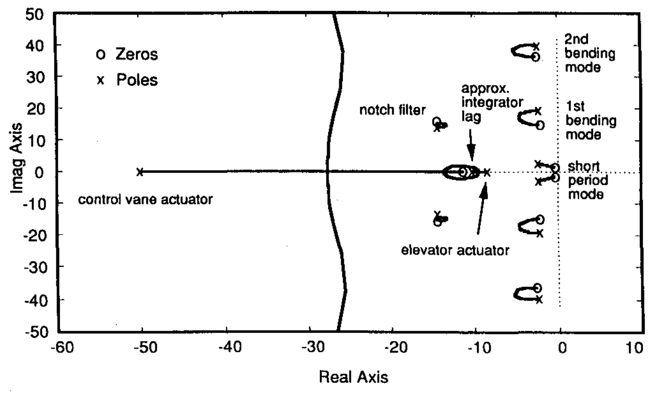

Fig. 2 SMCS root locus.

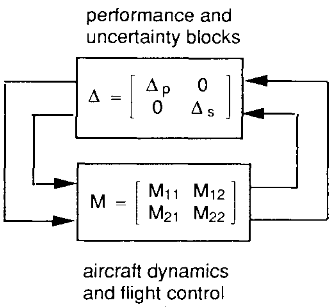

Fig. 3 Standard structured singular value analysis diagram.

The resulting SAS/SMCS control system is very simple in structure, consisting of three gains and two filters. The control system is multivariable because three feedback signals are used in conjunction with two control effectors. However, the control system was designed by sequentially closing the feedback loops of the SAS and SMCS. The control system robustness evaluation will be conducted in the following sections of this paper assuming uncertainty occurs in both feedback loops simultaneously.

III. Review of Structured Singular Value Analysis

The structured singular value analysis technique provides a tool that can measure robust stability and robust performance of a multivariable control system. The structured singular value analysis technique was developed initially by Doyle[9-11] and has received wide acceptance. Consequently, the structured singular value analysis technique provides an ideal tool to form and test multivariable flight control system evaluation guidelines.

The structured singular value analysis technique requires construction of a special block diagram for analysis. The most general form of the diagram is shown in Fig. 3. Model uncertainty is represented by the block Δ_S, whereas a robust performance requirement is represented by the block Δ_p. The Δ matrix is defined by

$$\Delta = \begin{pmatrix} \Delta_p & 0 \\ 0 & \Delta_S \end{pmatrix} \tag{1}$$

The transfer function matrix M, defined by

$$M = \begin{pmatrix} M_{11} & M_{12} \\ M_{21} & M_{22} \end{pmatrix} \tag{2}$$

represents the aircraft and flight control system transfer function components "seen" by the uncertainty and performance requirements contained in Δ.

Doyle has shown that, assuming nominal stability, the control system will be stable for all uncertainty Δ_S whose maximum singular value is bounded by

$$\bar{\sigma}(\Delta_S) < \alpha_S \tag{3}$$

where α_S is defined as the inverse of the maximum structured singular value $\mu_{\max}$ (with M_{22} evaluated over positive frequencies), or

$$\alpha_S = \frac{1}{\mu_{\max}(M_{22})} \tag{4}$$

The structured singular value μ takes into account the "structure" of the model uncertainty through the definition of Δ. For the cases addressed in this paper, the model uncertainty and performance requirements will be mutually exclusive so that Δ becomes a diagonal matrix of one-by-one blocks. The computation of μ involves scaling each of the one-by-one blocks to minimize conservatism of the robustness predictions. The Frobenius norm scaling technique[12] provides an approximate upper bound measure of the structured singular value and is used for all of the results reported in this paper. Because the scaling technique yields an upper bound, the results presented in this paper can be viewed as optimistic.

Robust performance is measured by including the structure of both Δ_S and Δ_p, which yields

$$\bar{\sigma}(\Delta) < \alpha_p \tag{5}$$

where

$$\alpha_p = \frac{1}{\mu_{\max}(M)} \tag{6}$$

Doyle's results can be used to provide a measure of stability robustness and performance robustness, through the parameters α_S and α_p, respectively. These measures can also be interpreted as evaluation guidelines. For example, a minimum value for α_S or α_p can be recommended and will be the subject of this paper.

IV. Analysis Block Diagram Construction

For this evaluation, a structured singular value analysis diagram will be constructed to reflect the specific design objectives of the ILAF control scheme. The design objectives are to maintain stability, transient response performance, and turbulence response performance in the presence of bounded model uncertainty. Figure 4 shows the complete evaluation diagram for the flexible aircraft robustness evaluation. Each δ in Fig. 4 represents either a bounded model uncertainty or a performance requirement. The definition and formulation of each δ will be discussed in the remainder of this section.

The current military flight control system specification recommends that stability robustness be measured using gain and phase margins in each control loop, with all of the other loops closed at their nominal gain values. The structured singular value technique can be used to measure stability robustness to gain and/or phase variations occurring simultaneously in all feedback loops. To measure stability robustness, a complex uncertainty parameter is inserted into each feedback loop of the closed-loop control system. Uncertainties will be placed in the control input paths (as opposed to the feedback response paths) for this evaluation. The uncertainty parameters δ_3 and δ_4 in Fig. 4 represent bounded modeling uncertainties in the elevator and control vane feedback paths, respectively. As a result, the uncertainty block Δ_S can be defined as

$$\Delta_S = \begin{pmatrix} \delta_3 & 0 \\ 0 & \delta_4 \end{pmatrix} \tag{7}$$

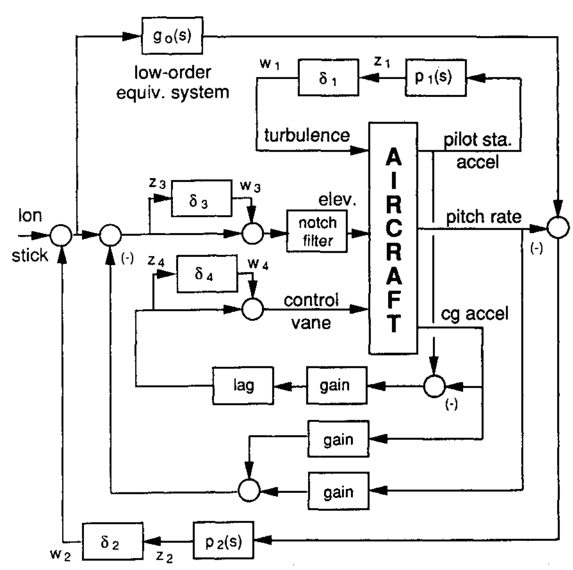

Fig. 4 Analysis diagram for the SAS/SMCS.

Typically, performance requirements cannot be described simply by a complex-valued parameter. In most cases, a weighting filter must be used to completely describe the performance requirement. A useful form for the performance specifications is

$$\|f(j\omega)p(j\omega)\|_\infty < 1 \tag{8}$$

where $f(s)$ is the system transfer function of interest, $p(s)$ is a performance weighting filter, and the $\|(\cdot)\|_\infty$ notation denotes the H^∞ norm or the largest maximum singular value over positive frequencies. Two performance requirements are considered, one related to the objective of the SMCS, which is to reduce the effect of turbulence, whereas the other is related to the purpose of the SAS, which is to augment the aircraft transient response. The performance block is then

$$\Delta_p = \begin{pmatrix} \delta_1 & 0 \\ 0 & \delta_2 \end{pmatrix} \tag{9}$$

Turbulence Response Performance

The objective of the SMCS is to shape the aircraft response at the cockpit location resulting from turbulence inputs. A plunge velocity turbulence input can be specified by a power spectral density Φ_w and an intensity σ_w^2. The power spectral density is usually defined by the Dryden form,[4]

$$\Phi_w(\omega) = \frac{2L_w}{V\pi}\frac{1+12(L_w\omega/V)^2}{\left[1+4(L_w\omega/V)^2\right]^2} \tag{10}$$

where the characteristic length L_w is here assumed to be 25 ft and $V = 942$ ft/s.

Assuming the transfer function from the turbulence input to the vertical acceleration at the aircraft cockpit is $f(s)$, the power spectral density for output, represented by Φ_{nzp}, is given by

$$\Phi_{nzp}(\omega) = |f(j\omega)|^2\Phi_w(\omega)\sigma_w^2 \tag{11}$$

The SMCS design objective might be described mathematically as the desire to shape the cockpit response power spectral density such that $\Phi_{nzp}(\omega) < r(\omega)$ for some frequency-dependent function $r(\omega)$. Wykes considered a design specification for the SMCS that intended to restrict the steady-state rms value of the pilot's head.[13] Consequently, the specification limited the amount of head motion due to turbulence so that the pilot could comfortably read the cockpit instruments. The SMCS performance requirement will have the form

$$V^2\frac{1}{\sigma_w^2}|T(j\omega)|^2\Phi_{nzp}(\omega) < r(\omega) \tag{12}$$

where $T(s)$ represents the transmission of acceleration through the vertical axis of the human body.

There has been some debate about the exact response of the human head when the body is excited by vertical vibrations.[14] Primarily, the differences in experimental data can be attributed to differences in experimental apparatus, input excitation, and seat characteristics. Nevertheless, most experimental data indicate a slight resonance near 4.5 Hz (28 rad/s). The human response function chosen for this study is

$$T(s) = \frac{28^2}{s^2+2(0.5)28s+28^2} \tag{13}$$

Using the previous human response transfer function, the design requirement becomes

$$V^2|T(j\omega)|^2|f(j\omega)|^2\Phi_w(\omega) < r(\omega) \tag{14}$$

The frequency weighting function $r(\omega)$ was chosen using Eq. (14) with $f(s)$ representing the aircraft response when only the SAS is operating. The function $r(\omega)$ is chosen as

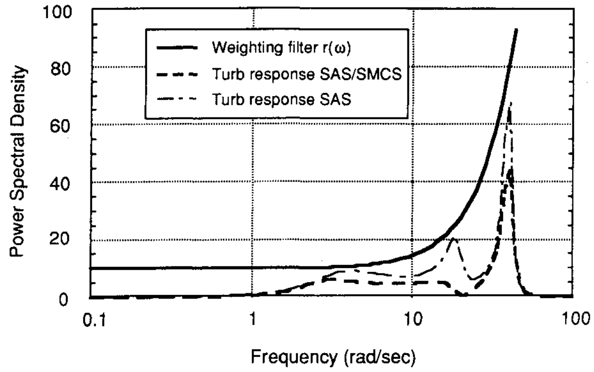

Fig. 5 Turbulence response weighting filter.

$$r(\omega) = (10/15^2)(15^2+\omega^2) \tag{15}$$

The weighting function $r(\omega)$ is shown as a solid line along with the left side of Eq. (14) for both the SAS only (dashed-dot line) and the SAS/SMCS (dashed line) in Fig. 5. Note that $r(\omega)$ is slightly larger than the SAS only response, whereas the SAS/SMCS response is much smaller than $r(\omega)$.

Equation (14) can also be written as

$$V^2|T(j\omega)|^2|f(j\omega)|^2\frac{\Phi_w(\omega)}{r(\omega)} < 1 \tag{16}$$

Equation (16) is in the appropriate form for implementation in the analysis diagram with the frequency response of a filter $p_1(s)$ chosen so that

$$|p_1(j\omega)|^2 = V^2|T(j\omega)|^2\frac{\Phi_w(\omega)}{r(\omega)} \tag{17}$$

A practical turbulence response performance weighting filter is then

$$p_1(s) = \frac{V(28)^2}{s^2+2(0.5)28s+28^2}\sqrt{\frac{2L_w}{V\pi}}\frac{1+2\sqrt{3}(L_ws/V)}{\left[1+2(L_ws/V)\right]^2} \times \frac{15}{\sqrt{10}(s+15)} \tag{18}$$

or

$$p_1(s) = \frac{16.7V^2(s+10.9)}{(s+18.8)^2\left[s^2+2(0.5)28s+28^2\right](s+15)} \tag{19}$$

Turbulence performance is represented in Fig. 4 by the path from w_1 to z_1 and the block δ_1.

Transient Response Performance

In a recent technical paper, authors Moorhouse and Kisslinger[15] remarked: "It is normal to assess the robustness of the design system stability in the face of plant uncertainty. It would be beneficial to conduct research into techniques for ensuring an analogous robustness with respect to purity of response."

The purity of response terminology in the previous quote refers to deviations from a "pure" second-order response required by the military flying qualities specifications. This remark also provides a motivation for investigating transient response performance robustness.

Many flying qualities requirements are based on parameters defining an equivalent low-order representation of the actual aircraft response. The error that results from the equivalent system formulation has been under study to determine the largest allowable mismatch. The current military flying qualities specification includes a requirement on the "added dy-

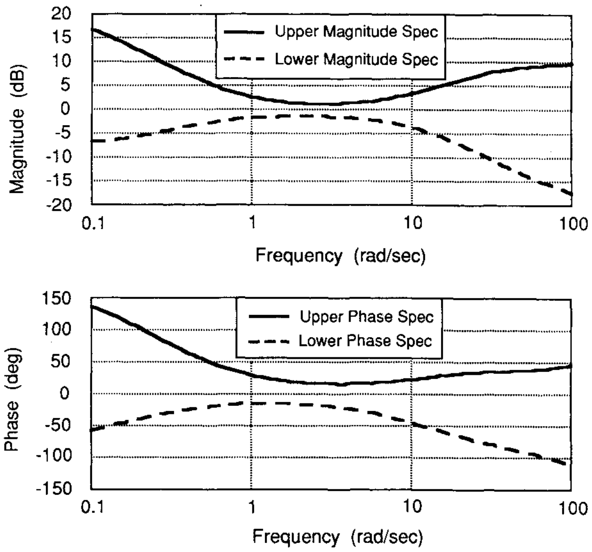

Fig. 6 Added dynamics specification.

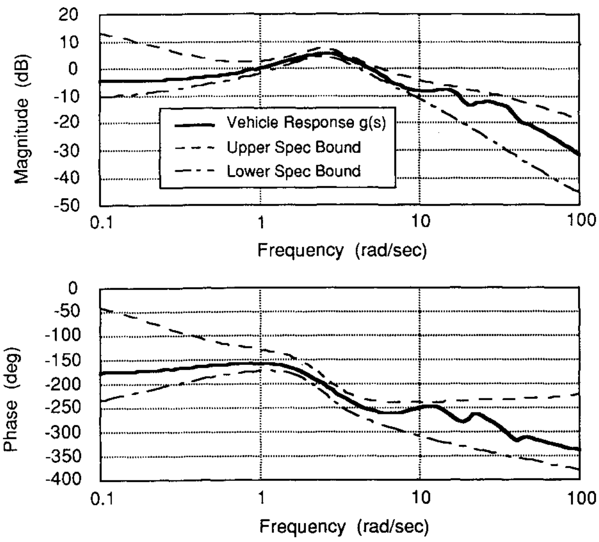

Fig. 7 Vehicle response inside specification.

namics" that frequently result from additional control system modes and can degrade pilot ratings. The specification was obtained by examining pilot rating differences between pairs of in-flight simulated responses that included various dynamic modes added to low-order equivalent models. Differences that resulted in a pilot rating change of one unit (Cooper-Harper scale) were used to define an envelope of maximum unnoticeable added dynamics.

The added dynamics includes any dynamics in the vehicle closed-loop response that are not represented in the equivalent system dynamics. Therefore, the added dynamics specification limits the deviation of the actual closed-loop response from the pure, low-order, equivalent system form. The added dynamics specification consists of upper and lower magnitude and phase bounds that are depicted in Fig. 6. The response of the added dynamics should lie inside the envelopes depicted in Fig. 6.

The upper and lower magnitude bounds of the added dynamics bounds are frequency-dependent functions. The upper bound $m_u(\omega)$ is defined by

$$m_u(\omega) = \left| \frac{3.16s^2 + 31.61s + 22.79}{s^2 + 27.14s + 1.84} \right|_{s=j\omega} \tag{20}$$

the lower bound $m_l(\omega)$ is expressed by

$$m_l(\omega) = \left| \frac{0.095s^2 + 9.92s + 2.15}{s^2 + 11.6s + 4.95} \right|_{s=j\omega} \tag{21}$$

As a measure of equivalent system mismatch, these magnitude bounds are applicable to longitudinal axis, pitch-rate response transfer functions as they were originally developed from NT-33 flight test data.[4] These frequency-dependent functions will be used herein as the "template" of a performance requirement that will limit the deviation of the closed-loop pitch-rate frequency response from a simplified, low-order equivalent model of the aircraft response.

A low-order equivalent model of the pitch-rate response of the aircraft (with SAS/SMCS closed) was found using the internally balanced model reduction algorithm.[16] The low-order equivalent model defines $g_0(s)$ as

$$g_0(s) = \frac{K_q(s + 1/\tau_{\theta 2})}{s^2 + 2\zeta_{sp}\,\omega_{sp} s + \omega_{sp}^2} \tag{22}$$

where $K_q = -4.0$ (rad/s^2), $1/\tau_{\theta 2} = 1.06$ (1/s), $\zeta_{sp} = 0.43$, and $\omega_{sp} = 2.53$ (rad/s). Figure 7 shows the nominal closed-loop pitch-rate frequency response $g(j\omega)$ inside the added dynamics specification. Note that the peaks at high frequency are due to the bending modes of the aircraft. The magnitude of these peaks and their subsequent effect on the aircraft response to pilot commands motivated the addition of the 20 rad/s notch filter in the elevator loop of the SAS/SMCS design.

The added dynamics specification will be used as a template for a flying qualities robust performance requirement. The specification will be interpreted for this research as a bound on how far the vehicle response can vary due to modeling uncertainty before the pilot rating will be affected. The added dynamics specification magnitude can be written in the following form:

$$m_l(\omega)|g_0(j\omega)| < |g(j\omega)| < |g_0(j\omega)|m_u(\omega) \tag{23}$$

where $g(s)$ is the aircraft pitch-rate response from the longitudinal stick input and $g_0 6(s)$ is the low-order equivalent of $g(s)$.

By adding and subtracting $g_0(j\omega)$ to Eq. (23), the following equation results:

$$m_l(\omega)|g_0(j\omega)| < |g_0(j\omega) - [g_0(j\omega) - g(j\omega)]| < |g_0(j\omega)|m_u(\omega) \tag{24}$$

If $|g_0(j\omega)| > |g_0(j\omega) - g(j\omega)|$, then the left side of the inequality (24) is satisfied if

$$m_l(\omega)|g_0(j\omega)| < |g_0(j\omega)| - |g_0(j\omega) - g(j\omega)| \tag{25}$$

Solving for the difference between $g_0(j\omega)$ and $g(j\omega)$ yields

$$|g_0(j\omega) - g(j\omega)| < [1 - m_l(\omega)]|g_0(j\omega)| \tag{26}$$

or

$$|g_0(j\omega) - g(j\omega)| \left\{ \frac{1}{[1 - m_l(\omega)]|g_0(j\omega)|} \right\} < 1 \tag{27}$$

Similarly, the right side of the inequality (24) is satisfied if

$$|g_0(j\omega) - g(j\omega)| \left\{ \frac{1}{[m_u(\omega) - 1]|g_0(j\omega)|} \right\} < 1 \tag{28}$$

The requirements of the upper and lower magnitude bounds can be combined if one weighting filter $p_2(s)$ can be found such that

$$\frac{1}{[1 - m_l(\omega)]|g_0(j\omega)|} < |p_2(j\omega)|$$

and

$$\frac{1}{[m_u(\omega) - 1]|g_0(j\omega)|} < |p_2(j\omega)| \tag{29}$$

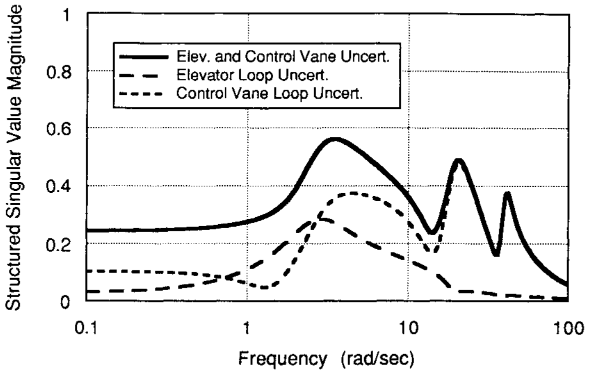

Fig. 8 Stability robustness structured singular values.

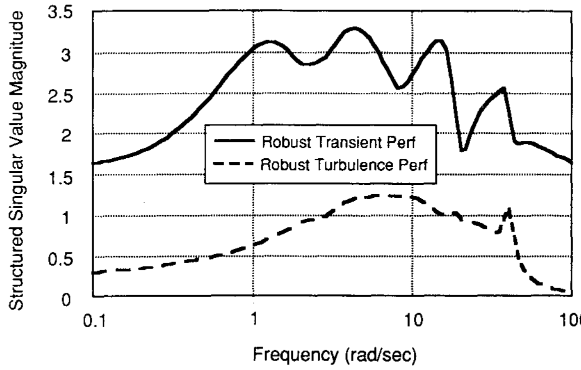

Fig. 9 Performance robustness structured singular values.

The transient response performance weighting filter was chosen from Eq. (29) and is

$$p_2(s) = \frac{(s^2+2.176s+6.4)(1.17s^2+29.63+7.33)}{4(s+1.06)(s^2+4.1s+4.4)(1000s+1)} \tag{30}$$

Transient response performance is represented in the analysis diagram of Fig. 4 by the path from w_2 to z_2, which includes the performance block δ_2.

V. Robust Stability Evaluation Results

The stability robustness characteristics of the SAS/SMCS system are determined by computing the structured singular values of M_{22}, where M_{22} is defined by

$$\begin{pmatrix} z_3 \\ z_4 \end{pmatrix} = M_{22}\begin{pmatrix} w_3 \\ w_4 \end{pmatrix} \tag{31}$$

The structured singular values of M_{22} are shown as the solid line in Fig. 8. The peaks evident in the structured singular value curve correspond roughly to the aircraft short period (2.6 rad/s) and the first (19.7 rad/s) and second (40.0 rad/s) fuselage bending modes in order of increasing frequency. The maximum structured singular value of $\mu_{\max}(M_{22}) = 0.56$ occurs near 3.0 rad/s and defines the stability robustness parameter $\alpha_S = 1/0.56 = 1.8$. For reference, the long dashed line in Fig. 8 shows the singular value curve for the case when only elevator loop uncertainty δ_3 is considered, whereas the short dashes depict the case when only control vane loop uncertainty δ_4 is considered. It is interesting to note that the elevator loop is most affected by uncertainty near the short-period natural frequency, and it is hardly affected at all by uncertainty near the structural mode frequencies. The control vane loop is most affected by uncertainty near the first bending mode frequency with significant peaks also occurring near the short-period and second bending mode frequencies.

Many researchers have interpreted the stability robustness parameter as an equivalent multiloop gain and phase (stability) margin.[17,18] The positive gain margin GM_{pos} is usually defined by

$$GM_{\text{pos}} = 1 + \alpha_S \tag{32}$$

whereas the negative gain margin GM_{neg} is defined by

$$GM_{\text{neg}} = 1 - \alpha_S \tag{33}$$

where α_S is less than one. The multiloop phase margin is defined by

$$PM = \pm\cos^{-1}\left(\frac{2-\alpha_S^2}{2}\right) \tag{34}$$

For the SAS/SMCS, the stability robustness guideline is a positive gain margin of $GM_{\text{pos}} = +8.9$ dB and phase margin of $PM = \pm 125$ deg. The negative gain margin is not defined in this case because α_S is greater than one. As mentioned previously, both loops of the SAS/SMCS can be opened completely without causing an instability because the open-loop system is stable.

Because computation of the structured singular value is somewhat complicated and algorithms are not yet standardized, it may be more useful to reformulate the robustness guidelines into a form that does not require the structured singular value. The translation is fairly easy for the stability robustness guidelines. Given a specification on the allowable value of α_S, verification of the gain margin guidelines can be obtained by randomly varying the loop gain in each feedback loop within the range of $(1-\alpha_S, 1+\alpha_S)$ and computing the eigenvalues of the perturbed closed-loop system.[19] Verification of the phase margin guidelines can be made by repeated computation of the system return difference matrix determinant.

In summary, this evaluation reveals that flight control systems similar to the SAS/SMCS should have a positive gain margin of 8.9 dB and phase margin of ±125 deg in each feedback loop. For new aircraft or design studies, this guideline can be verified by repeatedly varying each loop gain or phase and checking system stability. Alternatively, the stability margins could be verified by computing the structured singular values of M_{22} and showing that the inverse of the maximum structured singular value is greater than $\alpha_S = 1.8$.

VI. Robust Performance Evaluation Results

Turbulence Response Performance

The structured singular values that measure robust turbulence response performance are shown as the dashed line in Fig. 9. Robust turbulence response performance is measured by computing the structured singular values of the M matrix defined by

$$\begin{pmatrix} z_1 \\ z_3 \\ z_4 \end{pmatrix} = M\begin{pmatrix} w_1 \\ w_3 \\ w_4 \end{pmatrix} \tag{35}$$

Robust turbulence response performance is measured from the peak value $\mu_{\max}(M)$ of the structured singular value curve shown as the dashed curve in Fig. 9. The peak occurs near 8 rad/s and has a value of $\mu_{\max}(M) = 1.2$. The peak also defines the turbulence performance robustness parameter α_p by

$$\bar{\sigma}(\Delta) < \alpha_p = \frac{1}{\mu_{\max}(M)} = 0.83 \tag{36}$$

The robust performance guidelines can also be translated into a form that does not require the computation of the structured singular value for verification. Recall that each performance weighting filter was chosen using form

$$\|f(j\omega)p(j\omega)\|_\infty < 1 \tag{37}$$

assuming $f(j\omega)$ includes no uncertainty. The maximum structured singular value determines a value of α_p such that

$$\alpha_p \| f(j\omega) p(j\omega) \|_\infty < 1 \tag{38}$$

when $f(j\omega)$ includes an uncertainty bounded by α_p. The factor α_p measures the amount of degradation in performance expected from feedback loop uncertainty.

The new robust turbulence response requirement is obtained by interpreting the factor α_p as a modification of the nominal weighting filter $p(s)$ to account for the performance degradation caused by uncertainty. Rewriting Eq. (38) as

$$\| f(j\omega) \alpha_p p(j\omega) \|_\infty < 1 \tag{39}$$

one can see that the new performance robustness requirement is simply the nominal performance requirement multiplied by the value of α_p.

The new turbulence response robust performance requirement is most easily expressed by Eq. (14) with $r(\omega)$ replaced by $(1/\alpha_p)r(\omega)$,

$$V^2 |T(j\omega)|^2 |f(j\omega)|^2 \Phi_w(\omega) < (1/\alpha_p) r(\omega) \tag{40}$$

or

$$V^2 |T(j\omega)|^2 |f(j\omega)|^2 \Phi_w(\omega) < \frac{1}{\alpha_p} \frac{10}{15^2} (15^2 + \omega^2) \tag{41}$$

Figure 10 shows the new turbulence response robust performance guideline with $\alpha_p = 0.83$ as the dashed line. The nominal performance filter is shown as the dash-dot line. Note that the robust performance requirement is larger (more lenient) than the nominal requirement.

The turbulence performance robustness guideline essentially states that the turbulence response performance can degrade by a factor of 0.83, with complex uncertainty of magnitude less than 0.83 introduced into each feedback loop. To compare this interpretation to the new guideline, the elevator loop gain was increased by a factor of 1.8, the control vane loop was decreased by a factor of 0.2, and the resulting cockpit power spectral density [left side of Eq. (41)] is shown as the solid line in Fig. 10. Note that the response of the closed-loop system with gain uncertainty violates the nominal performance requirement but lies below the robust performance requirement. The uncertainty limit can also be stated in terms of equivalent loop gain or phase using Eqs. (32–34) to produce equivalent loop gain uncertainty values of $+5.2$ and -15.4 dB and loop phase uncertainty of ± 49 deg.

To compare the turbulence performance robustness of a new control system with this example, the structured singular values of the M matrix defined in Eq. (35) can be computed. If the inverse of the maximum structured singular value is greater than 1.2 for the new design, one can claim that the turbulence performance robustness is improved over the SAS/SMCS example studied herein. Alternatively, the loop gain

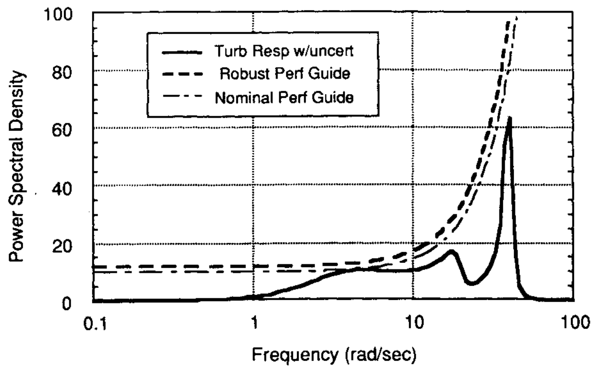

Fig. 10 Turbulence response robustness guideline.

of the feedback system can be varied between $+5.2$ and -15.4 dB or the phase varied in the range of ± 49 deg, and the frequency response of $V^2 |T(j\omega)|^2 |f(j\omega)|^2 \Phi_w(\omega)$ can be compared with the solid line in Fig. 10. As long as the frequency response of $V^2 |T(j\omega)|^2 |f(j\omega)|^2 \Phi_w(\omega)$ lies below the solid line for all gain and phase variations, the new system can be said to have equivalent (or better) turbulence performance robustness than the SAS/SMCS example.

Transient Response Performance

The structured singular values that measure robust transient response performance are shown as the solid line in Fig. 9. The M matrix for robust transient response performance is

$$\begin{pmatrix} z_2 \\ z_3 \\ z_4 \end{pmatrix} = M \begin{pmatrix} w_2 \\ w_3 \\ w_4 \end{pmatrix} \tag{42}$$

The maximum structured singular value of the dotted transient response performance robustness curve in Fig. 9 yields a value of $\mu_{\max}(M) = 3.3$. As a result, the transient response performance can degrade by a factor of 0.3 for loop gain uncertainty of $+2.3$ and -3.1 dB or loop phase uncertainty up to ± 17 deg.

The transient response performance robustness results can be translated into a frequency response envelope form. Recall that the transient response performance filter was chosen such that

$$\frac{1}{[1 - m_l(\omega)] |g_0(j\omega)|} < |p_2(j\omega)|$$

and

$$\frac{1}{[m_u(\omega) - 1] |g_0(j\omega)|} < |p_2(j\omega)| \tag{43}$$

Assuming that $p_2(s)$ was chosen to exactly match the nominal lower bound requirement $m_l(\omega)$, the new robust lower bound requirement $\hat{m}_l(\omega)$ is obtained from

$$\frac{1}{[1 - \hat{m}_l(\omega)] |g_0(j\omega)|} = \alpha_p |p_2(j\omega)| = \alpha_p \frac{1}{[1 - m_l(\omega)] |g_0(j\omega)|} \tag{44}$$

Solving for $\hat{m}_l(\omega)$ yields

$$\hat{m}_l(\omega) = 1 + (1/\alpha_p)[m_l(\omega) - 1] \tag{45}$$

Similarly, the upper bound of the new robust performance requirement is

$$\hat{m}_u(\omega) = 1 + (1/\alpha_p)[m_u(\omega) - 1] \tag{46}$$

Therefore, the new robust transient response performance guideline can be written in terms of the nominal added dynamics specification,

$$\begin{aligned} &\{1 + (1/\alpha_p)[m_l(\omega) - 1]\} |g_0(j\omega)| < |g(j\omega)| \\ &< |g_0(j\omega)| \{1 + (1/\alpha_p)[m_u(\omega) - 1]\} \end{aligned} \tag{47}$$

Note that Eq. (47) is the same as Eq. (23) when $\alpha_p = 1$.

Figure 11 shows the robust transient response performance guidelines for $\alpha_p = 0.3$. The solid line in Fig. 11 is the vehicle response with a gain uncertainty of 0.7 magnitude placed in both the elevator and control vane input paths. Note that the vehicle model with uncertainty lies within the predicted robust performance response bounds. The vehicle response with uncertainty would most certainly violate the nominal added dynamics specification bounds.

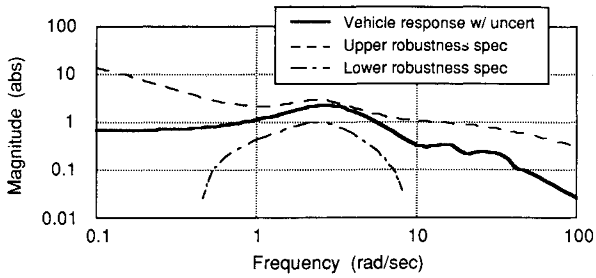

Fig. 11 Transient response robustness guideline.

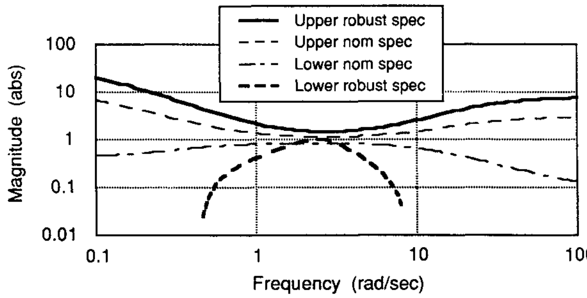

Fig. 12 Robust and nominal added dynamics specification comparison.

It is interesting to compare the original added dynamic specification to the new robust performance guideline. This comparison is made in Fig. 12 where the new guideline is represented by the heavy lines and the added dynamics specification is shown by the finer lines. One can clearly see the larger envelope defined by the robustness guideline, which allows for a limited amount of performance degradation due to model uncertainty.

To summarize the transient response performance guideline results, the inverse of the maximum structured singular value of the M matrix defined in Eq. (42) must be larger than 0.3 for a new design to have improved transient response performance over the SAS/SMCS. Verification of this performance level could also be obtained by repeatedly varying the feedback loop gain in the range of $+2.3$ and -3.1 dB or the loop phase in the range of ± 17 deg and by checking that the magnitude of the closed-loop pitch-rate response lies inside the envelopes depicted in Fig. 11.

VII. Conclusion

The results of this evaluation establish stability and performance robustness guidelines for large, flexible aircraft flight control systems. Unfortunately, without a basis for comparison, one cannot assign a relative merit to the reported robustness levels. However, the reported guidelines can be used to compare new control system designs to a control system that was designed using proven, successful design concepts.

Perhaps the most important contribution of this research is in the construction of structured singular value analysis diagrams using design objectives specific to flight control systems. In particular, performance weighting filters were generated for turbulence and transient response objectives using concepts from flight control and flying qualities studies. As a result, one can conclude that at least some of the past flight control experience gained over the years and documented in the military specifications can be used to formulate new guidelines for control systems designed specifically to improve robustness characteristics.

References

[1]Military Specification, Flight Control System, MIL-F-87242, March 1986.

[2]Anderson, M. R., Rabin, U. H., and Vincent, J. H., "Evaluation Methods for Complex Flight Control Systems," AIAA Guidance, Navigation, and Control Conference (Boston, MA), Aug. 1989 (AIAA Paper 89-3502).

[3]Paduano, J. D., and Downing, D. R., "Sensitivity Analysis of Digital Flight Control Systems Using Singular-Value Concepts," *Journal of Guidance, Control, and Dynamics,* Vol. 12, No. 3, 1989, pp. 297–303.

[4]Military Standard, Flying Qualities of Piloted Aircraft, MIL-STD-1797(USAF), March 1987.

[5]Krause, J., Morton, B., Enns, D., Stein, G., Doyle, J., and Packard, A., "A General Statement of Structured Singular Value Concepts," *Proceedings of the American Control Conference* (Atlanta, GA), Inst. of Electrical and Electronics Engineers, Piscataway, NJ, June 1988, pp. 389–393.

[6]Balas, G., Doyle, J., Glover, K., Packard, A., and Smith, R., *μ-Analysis and Synthesis Toolbox User's Guide,* MUSYN, Inc., and The Mathworks, Inc., Natick, MA, 1991.

[7]Salzwedel, H., and Vincent, J. H., "Modeling, Identification, and Control of Flexible Aircraft," Air Force Wright Aeronautical Lab., AFWAL-TR-84-3032, Wright-Patterson AFB, OH, Oct. 1983.

[8]Wykes, J. H., "Structural Dynamic Stability Augmentation and Gust Alleviation of Flexible Aircraft," AIAA 5th Annual Meeting (Philadelphia, PA), Oct. 21–24, 1968 (AIAA Paper 68-1067).

[9]Doyle, J. C., "Analysis of Feedback Systems with Structured Uncertainties," *IEE Proceedings,* Vol. 129, Pt. D, No. 6, 1982, pp. 242–249.

[10]Doyle, J. C., "Performance and Robustness Analysis for Structured Uncertainty," *21st IEEE Conference on Decision and Control* (Orlando, FL), Inst. of Electrical and Electronics Engineers, Piscataway, NJ, Dec. 1982, pp. 629–636.

[11]Doyle, J. C., "Structured Uncertainty in Control System Design," *24th IEEE Conference on Decision and Control* (Ft. Lauderdale, FL), Inst. of Electrical and Electronics Engineers, Piscataway, NJ, Dec. 1985, pp. 260–265.

[12]Osborne, E. E., "On Pre-Conditioning of Matrices," *Journal of the Association for Computing Machinery,* Vol. 7, 1960, pp. 338–345.

[13]Jones, J. G., "Ride-Bumpiness and the Influence of Active Control Systems," *High-Speed, Low-Level Flight: Aircrew Factors,* AGARD-CP-267, Oct. 1979, pp. 1-(1–16).

[14]Vogt, L., Schwartz, E., and Mertens, H., "Head Movements Induced by Vertical Vibrations," *High-Speed, Low-Level Flight: Aircrew Factors,* AGARD-CP-267, Oct. 1979, pp. 10-(1–13).

[15]Moorhouse, D. J., and Kisslinger, R. L., "Lessons Learned in the Development of a Multivariable Control System," National Aerospace and Electronics Conference, Dayton, OH, May 1989.

[16]Bacon, B. J., and Schmidt, D. K., "Fundamental Approach to Equivalent Systems Analysis," *Journal of Guidance, Control, and Dynamics,* Vol. 11, No. 6, 1988, pp. 527–534.

[17]Safonov, M. G., Laub, A. J., and Hartmann, G. L., "Feedback Properties of Multivariable Systems: The Role and Use of the Return Difference Matrix," *IEEE Transactions on Automatic Control,* Vol. AC-26, No. 1, 1981, pp. 47–65.

[18]Yeh, H., Ridgely, D. B., and Banda, S. S., "Nonconservative Evaluation of Uniform Stability Margins of Multivariable Feedback Systems," *Journal of Guidance, Control, and Dynamics,* Vol. 8, No. 2, 1985, pp. 167–174.

[19]Stengel, R. F., and Ray, L. R., "Stochastic Robustness of Linear Time-Invariant Control Systems," *IEEE Transactions on Automatic Control,* Vol. AC-36, No. 1, 1991, pp. 82–87.